biophysica

MDPI

Article

Immunological Effects of Cold Atmospheric Plasma-Treated Cells in Comparison with Those of Cells Treated with Lactaptin-Based Anticancer Drugs

Olga Troitskaya [1,*], Diana Novak [1,2], Mikhail Varlamov [1], Mikhail Biryukov [1,2], Anna Nushtaeva [1], Galina Kochneva [3], Dmitriy Zakrevsky [4,5], Irina Schweigert [6], Vladimir Richter [1] and Olga Koval [1,2,*]

1 Institute of Chemical Biology and Fundamental Medicine, Siberian Branch of the Russian Academy of Sciences, 630090 Novosibirsk, Russia
2 Department of Natural Sciences, Novosibirsk State University, 630090 Novosibirsk, Russia
3 State Research Center of Virology and Biotechnology "Vector", 630559 Koltsovo, Russia
4 Rzhanov Institute of Semiconductor Physic, Siberian Branch of the Russian Academy of Sciences, 630090 Novosibirsk, Russia
5 Department of Radio Engineering and Electronics, Novosibirsk State Technical University, 630090 Novosibirsk, Russia
6 Khristianovich Institute of Theoretical and Applied Mechanics, Siberian Branch of the Russian Academy of Sciences, 630090 Novosibirsk, Russia
* Correspondence: troitskaya_olga@bk.ru (O.T.); o.koval@niboch.nsc.ru (O.K.)

Abstract: The ability of dying cancer cells to induce an anticancer immune response can increase the effectiveness of anticancer therapies, and such type of death is termed immunogenic cell death (ICD). Cells can die along the ICD pathway when exposed not only to chemo- and immunotherapeutics, but also to various types of radiation, such as ionizing radiation and cold atmospheric plasma jets (CAP). We have previously shown that CAP, lactaptin, and a recombinant vaccinia virus encoding lactaptin induce in vitro molecular changes typical of ICD in cancer cells. In the current work, we treated MX-7 rhabdomyosarcoma cells with CAP and lactaptin-based anticancer drugs and evaluated the immunological effects of the treated cells. We showed that dendritic cells (DCs) captured cells treated with various ICD inducers with different efficiency. CAP-treated cells were weakly potent in inducing the maturation of DCs according to MHC II externalization. Moreover, CAP-treated cells were worse in the stimulation of IFN-α release in vitro and were poorly captured by spleen DCs in vivo. Under the irradiation conditions used, CAP was not capable of activating a significant immunological anti-tumor effect in vivo. It is possible that modifications of the CAP irradiation regimen will enhance the activation of the immune system.

Keywords: cold plasma jet; immunogenic cell death; dendritic cells; interferon

Citation: Troitskaya, O.; Novak, D.; Varlamov, M.; Biryukov, M.; Nushtaeva, A.; Kochneva, G.; Zakrevsky, D.; Schweigert, I.; Richter, V.; Koval, O. Immunological Effects of Cold Atmospheric Plasma-Treated Cells in Comparison with Those of Cells Treated with Lactaptin-Based Anticancer Drugs. *Biophysica* **2022**, *2*, 266–280. https://doi.org/10.3390/biophysica2030025

Academic Editors: Ricardo L. Mancera, Paul C Whitford and Chandra Kothapalli

Received: 10 August 2022
Accepted: 30 August 2022
Published: 1 September 2022

1. Introduction

Cold atmospheric plasma (CAP) is a near-room-temperature ionized gas, composed of reactive species, neutral particles and molecules, electrons, and other physical factors such as electromagnetic fields and weak UV and heating radiations [1]. Plasma interacts with organic materials such as cells without causing thermal/electric damage to the cell surface. CAP jets are promising tools for anticancer therapy, and strategies are being developed to translate this technology to the clinics. The efficiency of such treatment is associated with the viability of cancer cells after exposure to the CAP jet, which depends on the parameters of the plasma device operation. Nevertheless, the detailed mechanisms of CAP-irradiated cell death are poorly understood, and a detailed analysis of the cell death modalities activated by CAP treatment is required.

Currently, the search for novel antitumor agents that cause the death of cancer cells and activate the antitumor immune response is urgent. The use of immunogenic cell death (ICD)

inducers capable of triggering an antitumor immune response can significantly increase the effectiveness of anticancer therapies. The immunogenicity of dying cells can be determined by the activation of a certain combination of danger signals (DAMPs), which contributes to the recognition and uptake of these cells by antigen-presenting cells (APCs) [2]. The most important molecular markers indicating the induction of ICD include the exposure of calreticulin and the heat-shock protein HSP70 on the cell surface and the release of ATP and the non-histone, nuclear DNA-binding protein high-mobility group box 1 (HMGB1) to the intracellular space [3,4]. It has also been shown that the release of type I interferon (IFN) from dying tumor cells is an important factor in the induction of immunogenic cell death [2]. Type I IFN interacts with the IFNAR receptor, which consists of two subunits, IFNAR1 and IFNAR2, triggering the autocrine activation of IFN-I-related genes in tumor cells. Among these genes, that coding for the chemokine CXCL10 deserves special attention, as this molecule acts as an important chemotactic factor attracting immune cells to the tumor site. IFN-I causes an increase of the *cxcl10* gene expression and an accumulation of CXCL10 in the intercellular space of a tumor [5,6].

Cells with activated ICD markers are actively engulfed by phagocytic cells, and the processing and presentation of tumor antigens by dendritic cells triggers the activation of antigen-specific T lymphocytes, which leads to the stimulation of an adaptive immune response against tumor-associated antigens [2,7]. The uptake of dying cells by phagocytic cells is important for preventing inflammation and for generating a long-term antitumor response [8].

Antigen-presenting cells are cells of the immune system that can cleave protein antigens into peptides and present them in combination with major class histocompatibility complex (MHC) molecules on their surface to interact with their respective T cell receptors. Professional APCs include dendritic cells (DCs), macrophages, and B cells, while nonprofessional APCs comprise thymic epithelial cells and vascular endothelial cells involved in antigen presentation only for a short time [9]. Among the APCs, there are dendritic cells that are believed to play a main role in antigen presentation due to their ability to stimulate naive helper and cytotoxic T cells and perform antigen cross-presentation [10]. Dendritic cells are ubiquitous in tissues, where they perform their functions; however, most DCs originate from the red bone marrow. DCs are a rare population of immune cells; small populations of DCs are found in the spleen, thymus, blood, tonsils, skin, liver, lung, intestine, and lymph nodes [11,12]. Initially, dendritic cells are produced in an immature form. The encounter with an antigen and antigen processing and presentation are accompanied by DC maturation. Mature dendritic cells are characterized by the presence of surface costimulatory molecules, such as CD25, CD40, CD69, CD80, CD83, and CD86, as well as MHC II, which are necessary for the effective binding to T lymphocytes during antigen presentation [13]. Mature DCs migrate to the lymph nodes and stimulate naive T cells by binding to the T cell receptor [14]. Phagocytosis of apoptotic cells can activate the T cell immune response if the apoptotic cells emit specific DAMPs [15]. Thus, during the induction of immunogenic cell death in tumor cells, DAMPs are secreted and interact with receptors on DCs, stimulating their maturation. This interaction leads to an immune response that usually correlates with the formation of immunological memory [16]. The significant involvement of DCs in immune responses triggered by tumor cells during ICD induction has been described in various studies [17,18]. In this way, the ability of ICD inducers to stimulate an effective antitumor T cell response depends on the presence and predisposition to DC activation in the microenvironment of tumors [14].

Nowadays, some chemotherapeutic drugs, antitumor peptides, oncolytic viruses, and various physical methods of treating tumors are considered as the main inducers of immunogenic cell death [19–23]. The recombinant lactaptin analog RL2 [24], the recombinant vaccinia virus VV-GMCSF-Lact encoding human GM-CSF and lactaptin [25], and cold atmospheric plasma jets (CAP) [26–29] have also been shown to induce tumor cell death with signs of immunogenic death (ICD) in vitro [30–32]. In this work, we compared the immunological effects of tumor cells treated with either drugs based on lactaptin or CAP.

Although cold plasma has been extensively studied as a potential anti-tumor agent, only a few papers have examined the activation of immunogenic cell death under irradiation by CAP [33–35]. Nevertheless, such studies are very important because they help in the further optimization of clinical devices and treatment protocols. The comparative study we describe helps to partially fill the gaps in our understanding of the stages at which CAP-treated cells effectively activate the immune system, stimulating ICD effects.

2. Materials and Methods

2.1. Cell Lines and Mice

MX-7 murine rhabdomyosarcoma cells were obtained from the Russian cell culture collection (Russian Branch of the ETCS, St. Petersburg, Russia). MX-7 cells and immature dendritic cells were grown in Dulbecco's Modified Eagle's medium (DMEM, Sigma-Aldrich, St. Louis, MO, USA) or RPMI 1640 medium (Sigma-Aldrich, St. Louis, MO, USA) supplemented with 10% fetal bovine serum (GIBCO, Thermo Fisher, Waltham, MA, USA), 2 mM L-glutamine (GIBCO, Thermo Fisher, Waltham, MA, USA), 250 mg/mL of amphotericin B, and 100 U/mL of penicillin/streptomycin (GIBCO, Thermo Fisher, Waltham, MA, USA) in a humidified atmosphere containing 5% CO_2 at 37 °C. The cells were maintained as previously described [25].

Female C3H/He mice (6–8 weeks old) were obtained from the SPF vivarium of the Institute of Cytology and Genetics SB RAS, Novosibirsk, Russia.

2.2. Chemicals and Antibodies

RL2 was purified as described previously [36]. VV-GMCSF-Lact was constructed from L-IVP and purified as described previously [25]. The following chemicals and antibodies were obtained from commercial sources: CellTracker™ Green CMFDA Dye (Invitrogen, Carlsbad, CA, USA), CellTracker™ Red CMTPX Dye (Invitrogen, Carlsbad, CA, USA), anti-mouse CD11c-PE (Sony, San Jose, CA, USA), anti-mouse MHC II-FITC (Sony, San Jose, CA, USA), Tryple-Express (GIBCO, Thermo Fisher, Waltham, MA, USA), cisplatin (Veropharm, Moscow, Russia).

2.3. Cold Atmospheric Plasma System and Treatment Parameters

The plasma source of a cold plasma jet was described in [26,37]. The plasma source was a quartz discharge channel with a powered electrode inside and an external ring grounded electrode over the dielectric tube. A sinusoidal voltage signal with a frequency of ~52 kHz and an amplitude of up to 10 kV was applied to the electrodes. A dielectric capillary with a 2.3 mm diameter was placed into the excitation volume. When the voltage was applied to the electrodes, a discharge was ignited. Streamers formed near the powered electrode and propagated inside and outside of the plasma device, composing a visually uniform plasma jet. In the experiments, the effect of frequency self-organization of the streamer breakdown was realized; this caused the frequency of the current pulses registered on the target not to correspond to the frequency of the applied voltage [37]. Under the conditions of the present experiments, the frequency of the current pulses was ~13 kHz. Typical discharge parameter values were as follows: gas flow rate, v = 9 L/min, voltage amplitude, U = 4.9 kV, discharge current I, up to 12 mA, current half-width duration, 15 ns, average power, up to 0.2 W.

For the CAP treatment, 96-well plates with growing cells were placed on a stand of dielectric material so that the distance from the edge of the capillary to the liquid medium was 25 mm. The cells were cultivated in 100 µL of complete culture medium, and the fluid column above the cells was 3 mm. After CAP treatment, the plates were returned to the CO_2 incubator, and cultivation was continued under standard conditions.

2.4. Quantitative Determination of IFN-Alpha in Culture Medium

The concentration of interferon-alpha was analyzed in the cell culture medium by an enzyme immunoassay using a commercial IFN-alpha mouse ELISA kit (Invitrogen,

Carlsbad, CA, USA). The samples were prepared according to manufacturer's protocols, and optical density was measured with the multichannel spectrophotometer Apollo LB912 (Berthold Technologies, Bad Wildbad, Germany) at 450 nm (reference wavelength 620 nm). The data obtained were used to construct a calibration curve with the coordinates of optical density and concentration. The content of IFN-α in the samples was calculated from the calibration curve.

2.5. Bone Marrow-Derived Dendritic Cell Isolation

The isolation of dendritic cells was carried out similarly to the protocol described in [38]. Briefly, C3H/He mice were sacrificed by cervical dislocation, the femurs and tibias of the mice were cleaned from adjacent muscles and ligaments and treated with a 50% ethanol solution. The bones were incised in the distal parts in order to open the channel of the red bone marrow. The bone marrow cells were washed out of the canal with a cold PBS solution using a syringe. DC progenitors were obtained from the bone marrow of C3H/He mice by density gradient centrifugation through the Histopaque-1083 medium (Sigma, St. Louis, MO, USA). Immature DCs were generated by culturing DC progenitors in RPMI 1640 medium supplemented with 10% fetal bovine serum, 2 mM L-glutamine, 250 mg/mL of amphotericin B, and 100 U/mL of penicillin/streptomycin in the presence of 50 ng/mL of GM-CSF (Invitrogen, Carlsbad, CA, USA) and 50 ng/mL of IL-4 (Invitrogen, Carlsbad, CA, USA) in a humidified atmosphere containing 5% CO_2 at 37 °C for 3 days. After 3 days, half of the culture medium was removed from the flask and replaced with fresh RPMI 1640 growth medium, also supplemented with IL4 and GM-CSF, and cultivation was continued in a humidified atmosphere containing 5% CO_2 at 37 °C for 3 more days.

2.6. Flow Cytometry Analysis

All the tests were performed using the FACSCanto II flow cytometer (BD Biosciences, Franklin Lakes, NJ, USA), and the data were analyzed by FACSDiva Sofware Version 6.1.3. (BD Biosciences, Franklin Lakes, NJ, USA). The cultured cells were initially gated (P1) based on forward scatter versus side scatter to exclude small debris (Figure S1), and 10,000 events from this population were collected.

For CD11c and MHC II detection, the cells were incubated with primary anti-CD11c antibodies (1:100) or anti-MHC II antibodies (1:100) for 1 h at the room temperature. Rabbit IgG (Thermo Fisher Scientifc, Waltham, MA, USA) or mouse IgG (R&D, Minneapolis, MN, USA) were used as an isotype control.

2.7. Phagocytic Activity of Dendritic Cells

Immature dendritic cells were stained with 1 µM CellTracker™ Green CMFDA Dye for 30 min in a humidified atmosphere containing 5% CO_2 at 37 °C. Then, the cells were washed with PBS. Simultaneously, MX-7 cells growing in 6-well culture plates (TPP, Trasadingen, Switzerland) were incubated with 5 µM CellTracker™ Red CMTPX Dye for 30 min at 37 °C and then washed with PBS. The MX-7 cells were harvested with Tryple-Express, re-suspended in RPMI 1640 medium, and plated into 6-well culture plates with stained dendritic cells at the ratio of 1:1. After 3 h of incubation at 37 °C, cell samples were harvested with Tryple-Express, washed with PBS, and analyzed on the FACS CantoII flow cytometer. A double-positive population (Q2, double green–red glow) corresponded to dendritic cells that captured MX-7 cells.

2.8. Dendritic Cell Maturation

Immature dendritic cells were suspended in RPMI 1640 growth medium and mixed with MX-7 cells at a ratio of 1:1. The cell suspension was transferred into the wells of a 6-well plate and incubated for 18 h at 37 °C with 5% CO_2. Next, the cells were harvested with Tryple-Express and then stained with anti-CD11c and anti-MHC II antibodies. Cell

samples were analyzed on the FACS CantoII flow cytometer. Initial gating was performed on a population of CD11c-positive cells (Figure S2).

2.9. In Vivo Assay of MX-7 Tumor Cell Uptake by Spleen CD11c$^+$ Cells

MX-7 cells were incubated with 5 μM CellTracker™ Red CMTPX Dye for 30 min at 37 °C with 5% CO_2 and washed with PBS. After staining, MX-7 cells were incubated with RL2, or VV-GMCSF-Lact or irradiated with CAP, cultured for 24–48 h under standard conditions, and then harvested with Tryple-Express and washed with PBS. The cells were suspended in physiological saline and injected into C3H/He mice intravenously at a dose of 7×10^5 cells/mouse in 500 μL. After 3 h, the mice were sacrificed by cervical dislocation, and the spleens were removed. The spleens were weighed and then crushed with a glass homogenizer to obtain a cell suspension in RPMI 1640 medium (1 mL of medium per 50 mg of tissue). The spleen homogenates were filtered through a cell strainer (Falcon, Tewksbury, MA, USA) and centrifuged for 5 min at 200 g at room temperature, washed twice with PBS, and fixed for 10 min at room temperature with 10% formalin. The fixed cells were centrifuged for 5 min at 200 *g* and washed twice with PBS.

The fixed cells were stained with PE-conjugated anti-CD11c antibodies for 1 h at room temperature in the dark. After the incubation, cell samples were washed with PBS and analyzed on the FACS CantoII flow cytometer. The proportion of MX-7 cells stained with Cell Tracker Red was determined from the total number of CD11c$^+$ spleen cells.

2.10. Ethic Statement

All the animal experiments were carried out in compliance with the protocols and recommendations for the proper use and care of laboratory animals (EC Directive 86/609/EEC for animal experiments). The protocols were approved by the Committee on the Ethics of Animal Experiments of the Administration of the Siberian Branch of the Russian Academy of Science (Protocol Number 45, 16 November 2018). The mice were housed in ventilated animal cabinets under controlled lighting conditions at 65% humidity and 25 °C with a 10/14 h light–dark cycle and allowed food and water ad libitum. The animals were euthanized by cervical dislocation.

2.11. Statistics

Significance was determined using a two-tailed Student's *t*-test. A p value of less than 0.05 was considered significant. All the error bars represent the standard error of the mean. In mice experiment, the differences in tumor-free mice between groups were calculated using non-parametric statistics and Pearson's chi-square test and were significant for $p < 0.05$.

3. Results

3.1. Release of IFN-α into the Intercellular Space

In addition to major ICD markers, such as CRT or HMGB1, the release of type 1 interferon from treated cells has been shown to be important for the effective uptake of tumor antigens by dendritic cells. During the induction of immunogenic cell death, interferon-alpha (IFN-α), released from the dying cells, promotes the maturation of antigen-presenting cells, the cross-presentation of tumor antigens, and the recruitment of T cells [2].

The concentration of IFN-α was measured in the culture medium of MX-7 cells treated with RL2 (0.3 mg/mL), VV-GMCSF-Lact (VV, 0.5 PFU/cell), or a cold plasma jet (1 min, helium, voltage U = 4.9 kV, current I = 7 mA, pulse energy ~8 μJ). The culture medium was collected after 12 h (RL2), 48 h (VV), and 24 h (CAP) of treatment and analyzed by ELISA. The choice of the experimental points was based on the characteristic times of release of ATP and HMGB1 into the intercellular space following the stimulation with these inductors. Since tumor cells treated with the ICD inducer must emit DAMPs, they may not be cells in the final stage of death but may have passed the point of no return. Thus, earlier, it was

shown that RL2 caused the release of ATP and HMGB1 already after 12–24 h of incubation, CAP after 24 h, while the recombinant VV-GMCSF-Lact virus after 48 h [30–32].

IFN-α analysis of the treated cells showed that RL2 and the vaccinia virus VV-GMCSF-Lact caused a significant increase in the concentration of interferon-α in the culture medium up to 140 pg/mL and 80 pg/mL, respectively (Figure 1). Irradiation of cells with a cold plasma jet did not lead to an additional release of interferon from the treated cells relative to the control cells.

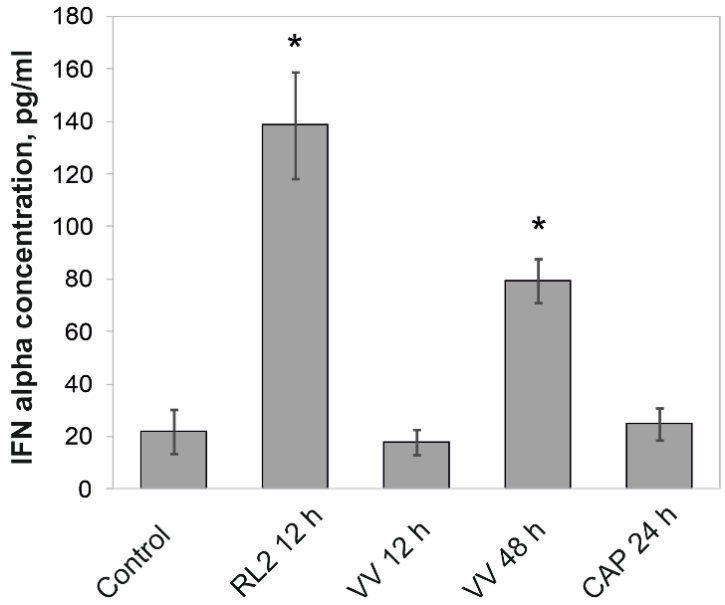

Figure 1. Change in the level of extracellular interferon-alpha (IFN-α) under the influence of RL2, VV-GMCSF-Lact (VV), and CAP. MX-7 cells were treated with RL2 (0.3 mg/mL, 12 h), VV (0.5 PFU/cell, 12 h and 48 h), or CAP (1 min, helium 9 L/min, 4.9 kV; 24 h after irradiation). Culture medium aliquots from the treated cells were analyzed by ELISA using an IFN-alpha mouse ELISA kit. Statistical differences between the control and the experimental groups are indicated by * for $p < 0.05$.

In terms of interferon secretion, the most significant cellular response occurred as a result of RL2 treatment, which could contribute to the vaccinating effect of RL2-treated cells in vivo observed in previous studies [30].

3.2. Phagocytosis of Tumor Cells Treated with ICD Inducers by Bone Marrow Dendritic Cells

Dendritic cells are the main antigen-presenting cells involved in the processing and presentation of tumor antigens to T lymphocytes for the establishment of an antitumor immune response upon induction of immunogenic cell death [14]. The efficient uptake of dying tumor cells by dendritic cells, as well as their subsequent maturation, is necessary to trigger the T cell antitumor immune response.

For the in vitro experiment of the dendritic cell uptake of tumor cells treated with ICD inducers, bone marrow dendritic cells from C3H/He mice were used. After the isolation of bone marrow progenitors of dendritic cells, PBMC were isolated and cultured according to the standard method in the presence of the cytokines GM-CSF and IL-4 for 6 days, after which the immature dendritic cells were used to evaluate the efficiency of tumor cell capture and for the analysis of DC maturation (Figure 2a). The proportion of $CD11c^+$ cells among the obtained immature dendritic cells was determined by flow cytometry after immunostaining with fluorescently labeled monoclonal antibodies against CD11c, one of the DC differentiation antigens. Approximately 90% of immature myeloid cells were found to carry the CD11c antigen on their surface, consistent with the dendritic cell phenotype (Figure 2b).

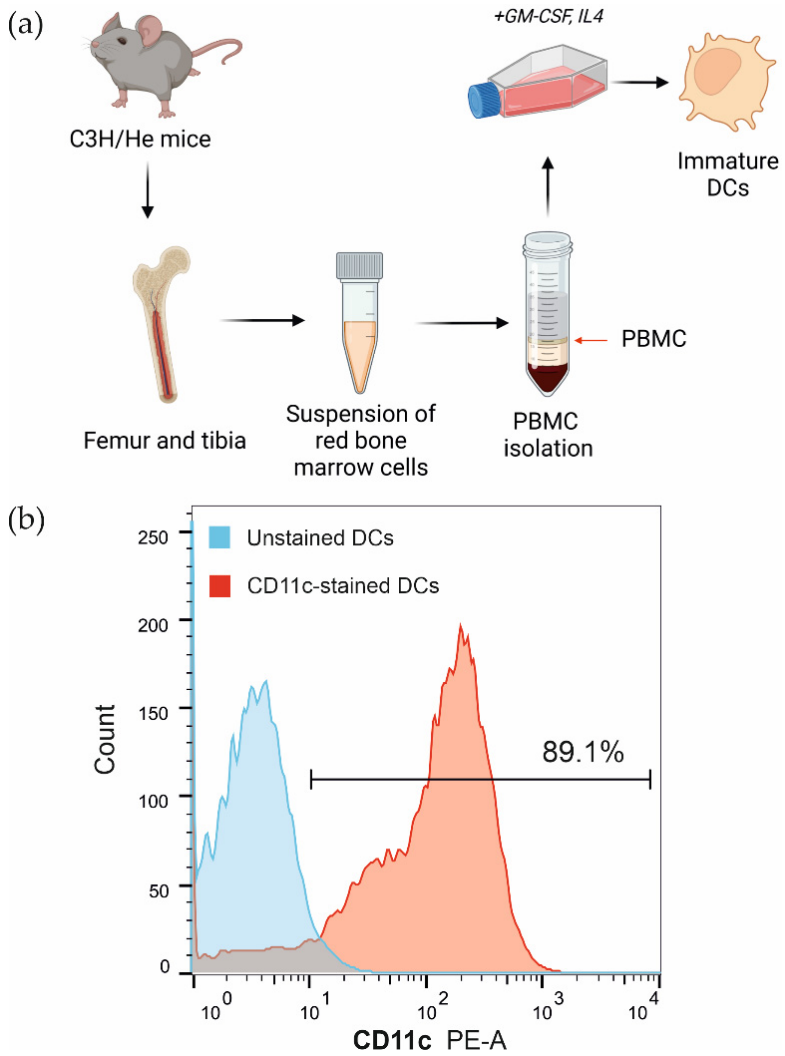

Figure 2. Immunophenotyping of PBMC isolated from the bone marrow of the femurs and tibias of C3H/He mice. (**a**) Scheme of the dendritic cell (DCs) isolation and cultivation. (**b**) Flow cytometry analysis of cells stained with fluorescently labeled anti-CD11c antibodies. A representative example of the analysis.

To induce cell death, MX-7 cells were treated with RL2 (0.3 mg/mL, 24 h), VV-GMCSF-Lact (0.5 PFU/cell, 48 h), or CAP (1 min, 24 h after irradiation). Then, the dying cells were stained with the fluorescent cytoplasmic dye Cell Tracker Red. The dendritic cells were stained with the Cell Tracker Green fluorescent dye (Figure 3a). Cisplatin (150 µM, 24 h) was used as a negative control drug that causes cell death but does not lead to the activation of ICD markers. DCs were incubated with dying MX-7 cells for 3 h and then analyzed by flow cytometry to evaluate the proportion of double-positive cells (Figure 3b, Q2 quadrant). The largest population of dendritic cells engulfing tumor cells or their fragments was found in samples with RL2-treated MX-7 cells (Figure 3b). There was no increase in the phagocytic DC population in samples containing cisplatin-treated cells compared to samples with untreated control cells. MX-7 cells infected with the virus were also phagocytosed by DCs; however, the increase in the double-positive population was not as significant as that measured with RL2-treated cells and amounted to 9.0%. The proportion of DCs that captured CAP-irradiated dying MX-7 cells was the smallest compared to those measured in the presence of virus- and RL2-treated cells (Figure 3b). Looking at the ratio of engulfed MX-7 cells to the total MX-7 cells added to DCs, more than 50% of the cells were taken up in the case of RL2 treatment, while only 13% of the cells were taken up in the case of CAP treatment (Figure 3c).

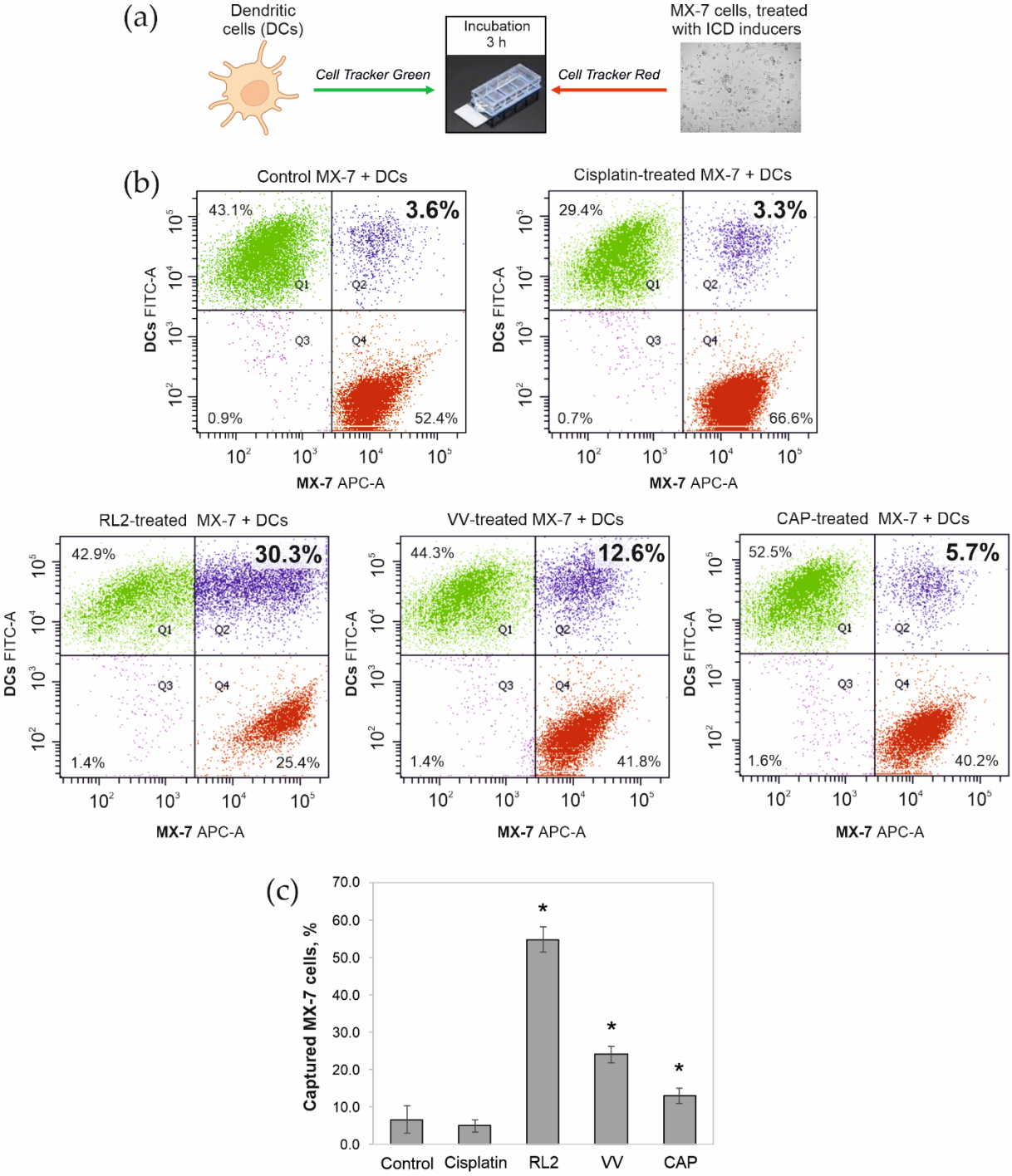

Figure 3. Phagocytosis of MX-7 cells by immature dendritic cells (DCs) from the red bone marrow of C3H/He mice. (**a**) Scheme of the experiment. MX-7 cells labeled with the Cell Tracker Red fluorescent dye (5 μM) were treated with RL2 (0.3 mg/mL, 24 h), VV-GMCSF-Lact (VV, 0.5 PFU/cell, 48 h), CAP (1 min, helium 9 L/min, 4.9 kV; 24 h after irradiation), or cisplatin (150 μM, 24 h). After treatment, the dying cells were incubated for 3 h with dendritic cells from the red bone marrow of C3H/He mice labeled with Cell Tracker Green (1 μM). (**b**) Representative images of the cytometric analysis. The quadrant Q2 contains a double-positive green/red population (phagocytosis). (**c**) Proportion of captured MX-7 cells. Statistical differences between control and experimental groups are indicated as * for $p < 0.05$.

3.3. Maturation of Bone Marrow Dendritic Cells after the Phagocytosis of Tumor Cells Treated with ICD Inducers

To evaluate the maturation of dendritic cells that had engulfed dying tumor cells, immature murine red bone marrow dendritic cells were incubated for 18 h with ICD inducer-treated MX-7 cells as described above. After the incubation, cell samples were stained with PE-conjugated CD11c and FITC-conjugated MHC II antibodies and analyzed by flow cytometry (Figure 4a). Initial gating was performed on a population of CD11c-positive cells to evaluate the MHC II-positive proportion in the dendritic cell population (Figure S2). The proportion of MHC II-positive cells was the highest in samples with RL2-treated MX-7 cells and was about 22% (Figure 4b). In samples incubated with cells irradiated with a cold plasma jet, the proportion of MHC II-positive cells was about 11%. DCs incubated with virus-infected or cisplatin-treated cells showed no signs of maturation (Figure 4c).

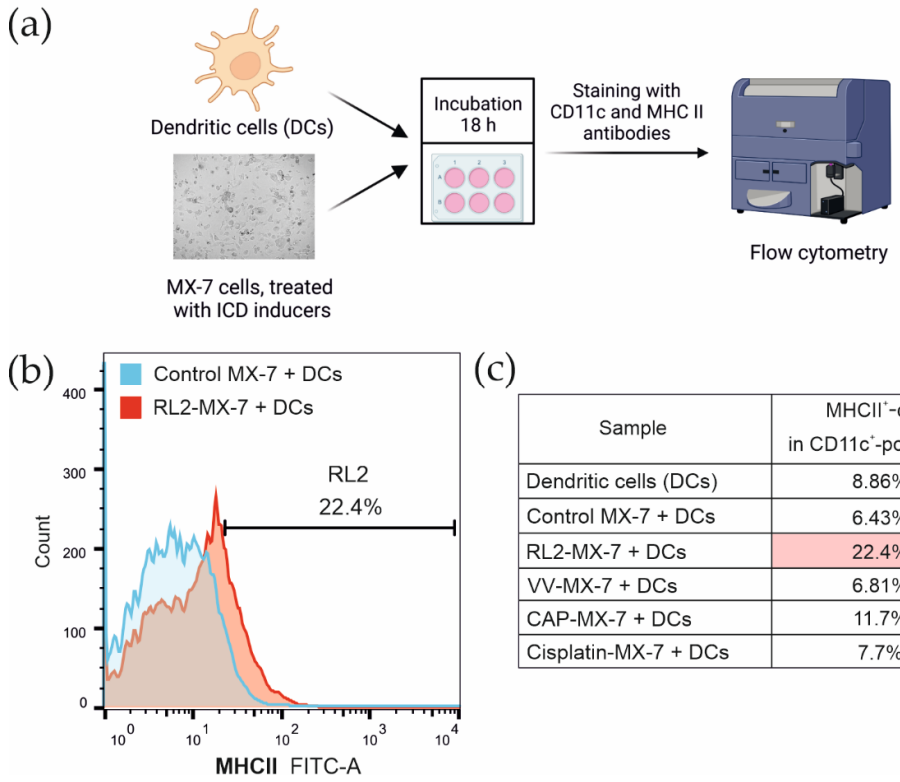

Sample	MHCII$^+$-cells in CD11c$^+$-population
Dendritic cells (DCs)	8.86%
Control MX-7 + DCs	6.43%
RL2-MX-7 + DCs	22.4%
VV-MX-7 + DCs	6.81%
CAP-MX-7 + DCs	11.7%
Cisplatin-MX-7 + DCs	7.7%

Figure 4. Maturation of bone marrow dendritic cells (DCs) form C3H/He mice after incubation with dying MX-7 tumor cells. (**a**) Scheme of the experiment. MX-7 cells were treated with RL2 (0.3 mg/mL, 24 h), VV-GMCSF-Lact (VV, 0.5 PFU/cell, 48 h), CAP (1 min, helium 9 L/min, 4.9 kV; 24 h after irradiation), or cisplatin (150 µM, 24 h). After treatment, MX-7 cells were incubated for 18 h with DCs from C3H/He mice. After the incubation, the samples were stained with PE-conjugated anti-CD11c antibodies and FITC-conjugated anti-MHC II antibodies and analyzed by flow cytometry. DCs without stimulation, stained with antibodies to CD11c, were used as an additional control. The analysis of the MHC II$^+$ cell populations was performed using CD11c$^+$ cells corresponding to the phenotype of DCs. (**b**) Proportion of the MHC II$^+$ cell population in relation to the total number of CD11c$^+$ cells in the sample containing control and RL2-treated cells. (**c**) Comparative proportion table of mature DCs (MHC II$^+$) in samples after activation by dying cells.

3.4. Capture of Tumor Cells by CD11c$^+$ Mouse Spleen Cells

Dendritic cell uptake of dying tumor cells was also investigated in an in vivo model. It is known that intravenous administration of UV-treated tumor cells leads to the capture of tumor cells by spleen DCs, which could be already detected after 3 h [39]. In our study, MX-7 cells were preliminarily stained with the Cell Tracker Red fluorescent dye and

incubated with RL2 or VV-GMCSF-Lact or irradiated with CAP, similarly to the experiment described above. After treatment, the dying tumor cells were injected intravenously into C3H/He mice. After 3 h, the mouse spleens were removed, a spleen cell suspension was prepared, and an immunostaining reaction was performed using a PE-conjugated antibody to CD11c antigen for DC detection (Figure 5a). Initial gating was performed on a population of CD11c-positive cells to evaluate the proportion of Cell Tracker Red (APC fluorescent channel)-labeled MX-7 cells, captured by $CD11c^+$ spleen DCs (Figure S3). As a result, tumor cell capture by spleen DCs was detected only in the spleens of animals injected with RL2-treated cells (Figure 5b,c). In spleen cell samples from mice injected with VV-GMCSF-Lact-treated or CAP-irradiated cells, there was no change in this population relative to control cells (Figure 5b,c).

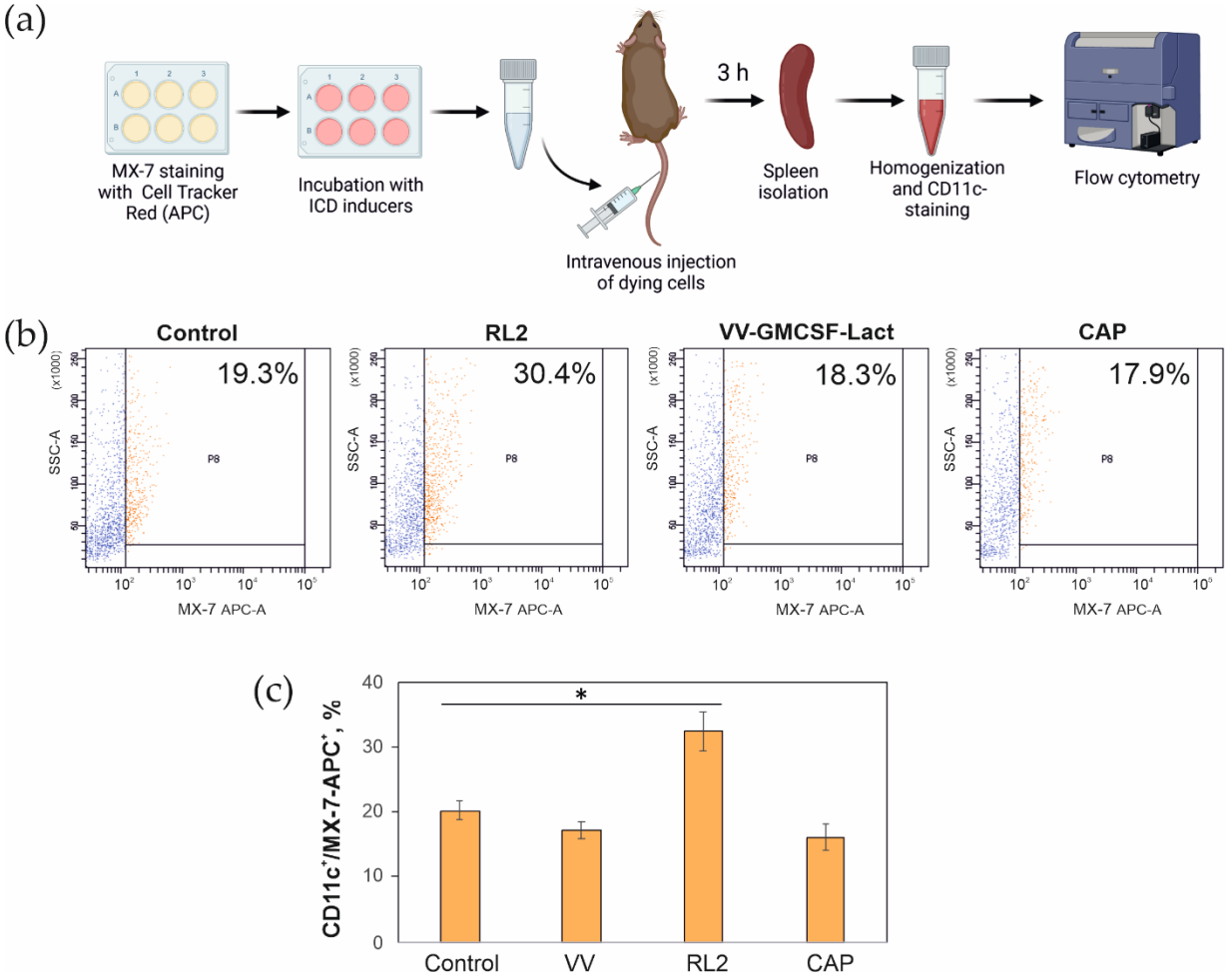

Figure 5. Capture of MX-7 tumor cells by $CD11c^+$ mouse spleen cells in vivo. (**a**) MX-7 cells were prestained with Cell Tracker Red (5 μM), treated with RL2 (0.3 mg/mL, 24 h) or VV-GMCSF-Lact (VV, 0.5 PFU/cell, 48 h), or irradiated with CAP (1 min, helium 9 L/min, 4.9 kV; 24 h after irradiation). After treatment, the dying cells were injected intravenously into C3H/He mice. After 3 h, the spleens were removed, crushed, stained with antibodies to CD11c, and analyzed by flow cytometry. (**b**) Representative images of the spleen APC^+ MX-7 uptake assay. The proportion of APC^+ cells is represented by the total number of $CD11c^+$ cells in the samples (APC: Ex = 650 nm, Em = 660 nm). (**c**) Average values of the $CD11c^+$ cell population which captured dying MX-7 cells. Data are presented as mean ± SD (n = 4). Statistical differences between control and experimental groups are indicated by * for $p < 0.05$.

4. Discussion

The last decade was marked by the emergence of the concept of immunogenic cell death (ICD), i.e., a form of cell death that stimulates an immune response against the antigens of dying cells, in particular, dying cancer cells. This model was first proposed in the context of cancer chemotherapy and has been supported by clinical data suggesting that a tumor-specific immune response may determine the efficacy of cancer therapies using conventional cytotoxic drugs. Since cancer is one of the most common causes of death among the working-age population worldwide, new approaches aimed at improving the methods of combating malignant neoplasms are highly relevant. Immunogenic cell death includes changes in the composition of the cell surface, as well as the release of soluble mediators, occurring in a certain time sequence. Such signals act on a number of receptors expressed on dendritic cells to stimulate the presentation of tumor antigens to T cells. Thus, it can be argued that ICD represents an important pathway for activating the immune system against tumor cells, which in turn determines the long-term success of anticancer therapies.

Although the activation of ICD markers by the CAP treatment of tumor cells has been shown in several studies, the activation of dendritic cells by CAP is still questionable. In a work [35], the researchers showed dendritic cells activation by cells treated with a combination of auranofin, a thioredoxin reductase 1 inhibitor, and a CAP-activated PBS solution. However, they showed no activation of DCs by a mono-treatment with CAP-activated PBS. Lin and co-authors demonstrated the emission of two danger signals: surface-exposed calreticulin and secreted adenosine triphosphate in A549 cells exposed to CAP irradiation [34]. Thus, our work contributes to the understanding of CAP-induced ICD at the level of the interaction of irradiated tumor cells with dendritic cells.

The literature does not show a direct release of IFN-α in response to a treatment with peptide-type ICD inducers, but it has been shown that the LTX-315 peptide, which activates ICD molecular markers in vitro, upregulates the expression of genes encoding type I interferons [40]. For vaccinia viruses, the literature shows the release of interferons upon infection with the recombinant vvDD virus [41]. Researchers showed that under the action of vvDD, type 1 IFN is released in different cell types at a concentration of 100 to 400 pg/mL, and, thus, the level of secretion of type 1 interferons in response to infection of the vvDD-type cells was comparable to that in cells infected with VV-GMCSF-Lact (80 pg/mL). It is known that interferons of the first type (IFN I) during the $CD8^+$ DCs capture of apoptotic tumor cells control the preservation of tumor antigens and are the optimal signal to activate the cross-presentation of antigens to T cells [39,42]. The obtained data indicating that the treatment of RL2 cells caused the highest release of interferon-alpha into the culture medium suggested a more efficient activation and a subsequent presentation of tumor antigens by dendritic cells that had absorbed such dying tumor cells to T cells and the establishment of a specific immune response. It is assumed that such stimulatory activity of IFN I against DCs is realized due to the fact that IFN I mimics the state of a viral infection or physiological stress, which are characteristic activators of the maturation of specific $CD8^+$ T cells [43]. It is worth noting that the lack of an interferon response to cold plasma jet irradiation is consistent with the weaker activation of other ICD molecular markers—CRT exposure, HSP70, and HMGB1 release—relatively to that observed with RL2 or VV-GMCSF-Lact treatment [30–32]. Based on the data on the release of IFN-α into the culture medium of cells treated with RL2 and VV-GMCSF-Lact, it can be assumed that such cells will be effective in DC stimulation.

We showed that the highest DC phagocytosis level was also observed in samples with RL2-treated MX-7 cells. It is believed that the efficiency of capture of dying tumor cells by dendritic cells correlates with their ability to present tumor antigens to T cells. So far, as it has been shown that RL2-treated cells possess vaccinating properties [30], it can be assumed that RL2-treated cells could stimulate the efficient capture and processing of tumor antigens in vivo, which would be accompanied by the establishment of a long-term antitumor immune response.

MHC II, or major histocompatibility complex type 2, is the main mediator of antigen presentation to T cells. While type I MHC molecules are expressed in almost all body cells except erythrocytes, type II MHC expression is characteristic of "professional" antigen-presenting cells, such as macrophages, B cells, and, especially, dendritic cells [44]. It is known that immature DCs have a low level of surface MHC II, and upon activation and maturation of dendritic cells, MHC II presence on the cell surface increases and is a marker of DC maturation [45]. It can be concluded that the previously observed capture of RL2-treated cells by dendritic cells was accompanied by the maturation of DCs. The observed weak stimulation of DCs by MX-7 cells infected with the VV-GMCSF-Lact could be a consequence of an indirect effect of the virus on DCs. It is known that specialized proteins of the vaccinia virus can not only block apoptosis at an early stage of infection [46], but also inhibit the maturation of dendritic cells. For example, the M2 protein synthesized by viruses in infected cells is secreted into the extracellular space and binds to CD80 molecules on DCs, blocking their maturation [47,48]. Thus, despite the observed capture by dendritic cells of MX-7 cells infected with VV-GMCSF-Lact (Figure 3b), such capture led to a weak activation of DC maturation (Figure 4b) and, accordingly, made the cascade of reactions leading to the establishment of a long-term immune response to tumor antigens less effective. The ineffectiveness of VV-treated MX-7 cells was also confirmed in a vaccination in vivo pilot study (Figure S4).

Based on our results, it can be concluded that, among the cells treated with potential ICD inducers, only RL2- and CAP-treated cells stimulated the maturation of dendritic cells.

5. Conclusions

The main purpose of the current study was to compare the immunological effects of MX-7 rhabdomyosarcoma cells treated with various potential inducers of ICD: a cold atmospheric plasma jet, a recombinant vaccinia virus, and the cytotoxic protein RL2. Among the studied inductors, RL2 caused the most significant changes in ICD-related signs, which agrees well with the observed in vivo effect of vaccination produced by RL2-treated tumor cells. CAP-treated cells were not capable of activating an anti-tumor immune response under the irradiation regimen used: they demonstrated poor IFN-α release, weakly stimulated their uptake by DCs, and showed low efficiency in supporting the maturation of DCs. It is possible that the CAP treatment conditions that stimulated ICD in vitro were not optimal for the activation of the immune system in vivo. Therefore, further investigation of CAP regimens to enhance the activation of the immune system is required.

Supplementary Materials: The following supporting information can be downloaded at: https://www.mdpi.com/article/10.3390/biophysica2030025/s1, Figure S1: Analysis of PBMC by flow cytometry in SSC/FSC graphs. These graphs were used to gate live cell population (P1) and to exclude debris; Figure S2: Gating on a population of CD11c-positive cells for the analysis of MHC II-positive cells. Representative images of RL2-treated MX-7 cells incubated with bone marrow dendritic cells. (a) CD11c-positive population; (b) MHC II-positive population among CD11c-positive cells; Figure S3: Gating on a population of CD11c-positive mouse spleen cells for analysis of Cell Tracker Red-stained cells. Representative image of spleen cells of mice injected with RL2-treated Cell Tracker Red MX-7 cells (APC fluorescent channel). (a) CD11c-positive population; (b) APC-positive population among CD11c-positive cells; Figure S4: Immunization of C3H/He mice with MX-7 cells treated with recombinant vaccinia virus VV-GMCSF-Lact (0.5 PFU/cell). (a) Scheme of the experiment. C3H/He mice were immunized with VV-GMCSF-Lact-treated MX-7 cells (7×10^5 cells/animal)—dot "0" on the x-axis. After 7 days, mice were injected with live MX-7 cells (7×10^5); (b) The number of live mice and mice without tumors in groups in dynamics. Differences between groups in the number of tumor- free mice were calculated using non-parametric Pearson's chi-square statistics. ns—differences between groups are not significant.

Author Contributions: Writing—original draft preparation, O.T. and O.K.; writing—review and editing, V.R. and I.S.; investigation, O.T., D.N., M.V., M.B. and A.N.; recombinant virus preparation, G.K.; supervision, D.Z. and O.K. All authors have read and agreed to the published version of the manuscript.

Funding: The authors gratefully acknowledge financial support from Russian Science Foundation grant # 19–19–00255-П (CAP experiments), Russian State-Funded Budget Project, grant number 121030200173-6 (cell culture works).

Data Availability Statement: Not applicable.

Acknowledgments: The authors would like to acknowledge Olga Chinak for the production and purification of RL2 and Elena Milakhina for help in the experiments with CAP. Figures 2, 4 and 5 were created with BioRender.com (accessed on 10 August 2022).

Conflicts of Interest: The authors declare no conflict of interest.

References

1. Lu, X.; Naidis, G.V.; Laroussi, M.; Reuter, S.; Graves, D.B.; Ostrikov, K. Reactive Species in Non-Equilibrium Atmospheric-Pressure Plasmas: Generation, Transport, and Biological Effects. *Phys. Rep.* **2016**, *630*, 1–84. [CrossRef]
2. Galluzzi, L.; Vitale, I.; Warren, S.; Adjemian, S.; Agostinis, P.; Martinez, A.B.; Chan, T.A.; Coukos, G.; Demaria, S.; Deutsch, E.; et al. Consensus Guidelines for the Definition, Detection and Interpretation of Immunogenic Cell Death. *J. Immunother. Cancer* **2020**, *8*, e000337. [CrossRef] [PubMed]
3. Zitvogel, L.; Apetoh, L.; Ghiringhelli, F.; Kroemer, G. Immunological Aspects of Cancer Chemotherapy. *Nat. Rev. Immunol.* **2008**, *8*, 59–73. [CrossRef] [PubMed]
4. Troitskaya, O.S.; Novak, D.D.; Richter, V.A.; Koval, O.A. Immunogenic Cell Death in Cancer Therapy. *Acta Nat.* **2022**, *14*, 40–53. [CrossRef]
5. Vacchelli, E.; Sistigu, A.; Yamazaki, T.; Vitale, I.; Zitvogel, L.; Kroemer, G. Autocrine Signaling of Type 1 Interferons in Successful Anticancer Chemotherapy. *Oncoimmunology* **2015**, *4*, e988042. [CrossRef]
6. Sistigu, A.; Yamazaki, T.; Vacchelli, E.; Chaba, K.; Enot, D.P.; Adam, J.; Vitale, I.; Goubar, A.; Baracco, E.E.; Remédios, C.; et al. Cancer Cell–Autonomous Contribution of Type I Interferon Signaling to the Efficacy of Chemotherapy. *Nat. Med.* **2014**, *20*, 1301–1309. [CrossRef]
7. Vacchelli, E.; Aranda, F.; Eggermont, A.; Galon, J.; Sautès-Fridman, C.; Cremer, I.; Zitvogel, L.; Kroemer, G.; Galluzzi, L. Trial Watch: Chemotherapy with Immunogenic Cell Death Inducers. *Oncoimmunology* **2014**, *3*, e27878. [CrossRef]
8. Fond, A.M.; Ravichandran, K.S. Clearance of Dying Cells by Phagocytes: Mechanisms and Implications for Disease Pathogenesis. In *Apoptosis in Cancer Pathogenesis and Anti-Cancer Therapy*; Gregory, C.D., Ed.; Advances in Experimental Medicine and Biology; Springer International Publishing: Cham, Switzerland, 2016; Volume 930, pp. 25–49. ISBN 978-3-319-39404-6.
9. Eiz-Vesper, B.; Schmetzer, H.M. Antigen-Presenting Cells: Potential of Proven und New Players in Immune Therapies. *Transfus. Med. Hemother.* **2020**, *47*, 429–431. [CrossRef]
10. Wculek, S.K.; Cueto, F.J.; Mujal, A.M.; Melero, I.; Krummel, M.F.; Sancho, D. Dendritic Cells in Cancer Immunology and Immunotherapy. *Nat. Rev. Immunol.* **2020**, *20*, 7–24. [CrossRef]
11. Puhr, S.; Lee, J.; Zvezdova, E.; Zhou, Y.J.; Liu, K. Dendritic Cell Development—History, Advances, and Open Questions. *Semin. Immunol.* **2015**, *27*, 388–396. [CrossRef]
12. Balan, S.; Saxena, M.; Bhardwaj, N. Dendritic Cell Subsets and Locations. In *International Review of Cell and Molecular Biology*; Elsevier: Amsterdam, The Netherlands, 2019; Volume 348, pp. 1–68. ISBN 978-0-12-818351-9.
13. Macri, C.; Fancke, B.; Radford, K.J.; O'Keeffe, M. Monitoring Dendritic Cell Activation and Maturation. In *Antigen Processing*; van Endert, P., Ed.; Methods in Molecular Biology; Springer: New York, NY, USA, 2019; Volume 1988, pp. 403–418. ISBN 978-1-4939-9449-6.
14. Lamberti, M.J.; Nigro, A.; Mentucci, F.M.; Rumie Vittar, N.B.; Casolaro, V.; Dal Col, J. Dendritic Cells and Immunogenic Cancer Cell Death: A Combination for Improving Antitumor Immunity. *Pharmaceutics* **2020**, *12*, 256. [CrossRef] [PubMed]
15. Garg, A.D.; Romano, E.; Rufo, N.; Agostinis, P. Immunogenic versus Tolerogenic Phagocytosis during Anticancer Therapy: Mechanisms and Clinical Translation. *Cell Death Differ.* **2016**, *23*, 938–951. [CrossRef] [PubMed]
16. Kepp, O.; Senovilla, L.; Vitale, I.; Vacchelli, E.; Adjemian, S.; Agostinis, P.; Apetoh, L.; Aranda, F.; Barnaba, V.; Bloy, N.; et al. Consensus Guidelines for the Detection of Immunogenic Cell Death. *Oncoimmunology* **2014**, *3*, e955691. [CrossRef] [PubMed]
17. Cirone, M.; Di Renzo, L.; Lotti, L.V.; Conte, V.; Trivedi, P.; Santarelli, R.; Gonnella, R.; Frati, L.; Faggioni, A. Activation of Dendritic Cells by Tumor Cell Death. *OncoImmunology* **2012**, *1*, 1218–1219. [CrossRef]
18. Di Blasio, S.; Wortel, I.M.N.; van Bladel, D.A.G.; de Vries, L.E.; Duiveman-de Boer, T.; Worah, K.; de Haas, N.; Buschow, S.I.; de Vries, I.J.M.; Figdor, C.G.; et al. Human CD1c^{+} DCs Are Critical Cellular Mediators of Immune Responses Induced by Immunogenic Cell Death. *Oncoimmunology* **2016**, *5*, e1192739. [CrossRef]

19. Casares, N.; Pequignot, M.O.; Tesniere, A.; Ghiringhelli, F.; Roux, S.; Chaput, N.; Schmitt, E.; Hamai, A.; Hervas-Stubbs, S.; Obeid, M.; et al. Caspase-Dependent Immunogenicity of Doxorubicin-Induced Tumor Cell Death. *J. Exp. Med.* **2005**, *202*, 1691–1701. [CrossRef]
20. Tesniere, A.; Schlemmer, F.; Boige, V.; Kepp, O.; Martins, I.; Ghiringhelli, F.; Aymeric, L.; Michaud, M.; Apetoh, L.; Barault, L.; et al. Immunogenic Death of Colon Cancer Cells Treated with Oxaliplatin. *Oncogene* **2010**, *29*, 482–491. [CrossRef]
21. Duewell, P.; Steger, A.; Lohr, H.; Bourhis, H.; Hoelz, H.; Kirchleitner, S.V.; Stieg, M.R.; Grassmann, S.; Kobold, S.; Siveke, J.T.; et al. RIG-I-like Helicases Induce Immunogenic Cell Death of Pancreatic Cancer Cells and Sensitize Tumors toward Killing by CD8+ T Cells. *Cell Death Differ.* **2014**, *21*, 1825–1837. [CrossRef]
22. Kim, J.H.; Oh, J.Y.; Park, B.H.; Lee, D.E.; Kim, J.S.; Park, H.E.; Roh, M.S.; Je, J.E.; Yoon, J.H.; Thorne, S.H.; et al. Systemic Armed Oncolytic and Immunologic Therapy for Cancer with JX-594, a Targeted Poxvirus Expressing GM-CSF. *Mol. Ther.* **2006**, *14*, 361–370. [CrossRef]
23. Turubanova, V.D.; Balalaeva, I.V.; Mishchenko, T.A.; Catanzaro, E.; Alzeibak, R.; Peskova, N.N.; Efimova, I.; Bachert, C.; Mitroshina, E.V.; Krysko, O.; et al. Immunogenic Cell Death Induced by a New Photodynamic Therapy Based on Photosens and Photodithazine. *J. Immunother. Cancer* **2019**, *7*, 350. [CrossRef]
24. Koval, O.A.; Fomin, A.S.; Kaledin, V.I.; Semenov, D.V.; Potapenko, M.O.; Kuligina, E.V.; Nikolin, V.P.; Nikitenko, E.V.; Richter, V.A. A Novel Pro-Apoptotic Effector Lactaptin Inhibits Tumor Growth in Mice Models. *Biochimie* **2012**, *94*, 2467–2474. [CrossRef] [PubMed]
25. Kochneva, G.; Sivolobova, G.; Tkacheva, A.; Grazhdantseva, A.; Troitskaya, O.; Nushtaeva, A.; Tkachenko, A.; Kuligina, E.; Richter, V.; Koval, O. Engineering of Double Recombinant Vaccinia Virus with Enhanced Oncolytic Potential for Solid Tumor Virotherapy. *Oncotarget* **2016**, *7*, 74171–74188. [CrossRef] [PubMed]
26. Schweigert, I.; Zakrevsky, D.; Gugin, P.; Yelak, E.; Golubitskaya, E.; Troitskaya, O.; Koval, O. Interaction of Cold Atmospheric Argon and Helium Plasma Jets with Bio-Target with Grounded Substrate Beneath. *Appl. Sci.* **2019**, *9*, 4528. [CrossRef]
27. Schweigert, I.; Alexandrov, A.; Zakrevsky, D.; Milakhina, E.; Patrakova, E.; Troitskaya, O.; Birykov, M.; Koval, O. Mismatch of Frequencies of Ac Voltage and Streamers Propagation in Cold Atmospheric Plasma Jet for Typical Regimes of Cancer Cell Treatment. *J. Phys. Conf. Ser.* **2021**, *2100*, 012020. [CrossRef]
28. Schweigert, I.; Alexandrov, A.; Zakrevsky, D.; Gugin, P.; Milakhina, E.; Golubitskaya, E.; Troitskaya, O.; Biryukov, M.; Koval, O. Analysis of Grounded Substrate Effects on Cold Atmospheric Plasma Jet Irradiation of Cellular and Animal Models. *J. Phys. Conf. Ser.* **2020**, *1698*, 012010. [CrossRef]
29. Golubitskaya, E.A.; Troitskaya, O.S.; Yelak, E.V.; Gugin, P.P.; Richter, V.A.; Schweigert, I.V.; Zakrevsky, D.E.; Koval, O.A. Cold Physical Plasma Decreases the Viability of Lung Adenocarcinoma Cells. *Acta Nat.* **2019**, *11*, 16–19. [CrossRef]
30. Troitskaya, O.; Varlamov, M.; Nushtaeva, A.; Richter, V.; Koval, O. Recombinant Lactaptin Induces Immunogenic Cell Death and Creates an Antitumor Vaccination Effect in Vivo with Enhancement by an IDO Inhibitor. *Molecules* **2020**, *25*, 2804. [CrossRef]
31. Koval, O.; Kochneva, G.; Tkachenko, A.; Troitskaya, O.; Sivolobova, G.; Grazhdantseva, A.; Nushtaeva, A.; Kuligina, E.; Richter, V. Recombinant Vaccinia Viruses Coding Transgenes of Apoptosis-Inducing Proteins Enhance Apoptosis But Not Immunogenicity of Infected Tumor Cells. *BioMed Res. Int.* **2017**, *2017*, 3620510. [CrossRef]
32. Troitskaya, O.; Golubitskaya, E.; Biryukov, M.; Varlamov, M.; Gugin, P.; Milakhina, E.; Richter, V.; Schweigert, I.; Zakrevsky, D.; Koval, O. Non-Thermal Plasma Application in Tumor-Bearing Mice Induces Increase of Serum HMGB1. *IJMS* **2020**, *21*, 5128. [CrossRef]
33. Khalili, M.; Daniels, L.; Lin, A.; Krebs, F.C.; Snook, A.E.; Bekeschus, S.; Bowne, W.B.; Miller, V. Non-Thermal Plasma-Induced Immunogenic Cell Death in Cancer. *J. Phys. D Appl. Phys.* **2019**, *52*, 423001. [CrossRef]
34. Lin, A.; Truong, B.; Patel, S.; Kaushik, N.; Choi, E.; Fridman, G.; Fridman, A.; Miller, V. Nanosecond-Pulsed DBD Plasma-Generated Reactive Oxygen Species Trigger Immunogenic Cell Death in A549 Lung Carcinoma Cells through Intracellular Oxidative Stress. *IJMS* **2017**, *18*, 966. [CrossRef] [PubMed]
35. Van Loenhout, J.; Freire Boullosa, L.; Quatannens, D.; De Waele, J.; Merlin, C.; Lambrechts, H.; Lau, H.W.; Hermans, C.; Lin, A.; Lardon, F.; et al. Auranofin and Cold Atmospheric Plasma Synergize to Trigger Distinct Cell Death Mechanisms and Immunogenic Responses in Glioblastoma. *Cells* **2021**, *10*, 2936. [CrossRef] [PubMed]
36. Semenov, D.V.; Fomin, A.S.; Kuligina, E.V.; Koval, O.A.; Matveeva, V.A.; Babkina, I.N.; Tikunova, N.V.; Richter, V.A. Recombinant Analogs of a Novel Milk Pro-Apoptotic Peptide, Lactaptin, and Their Effect on Cultured Human Cells. *Protein J.* **2010**, *29*, 174–180. [CrossRef] [PubMed]
37. Schweigert, I.V.; Alexandrov, A.L.; Zakrevsky, D.E. Self-Organization of Touching-Target Current with Ac Voltage in Atmospheric Pressure Plasma Jet for Medical Application Parameters. *Plasma Sources Sci. Technol.* **2020**, *29*, 12LT02. [CrossRef]
38. Markov, O.V.; Mironova, N.L.; Sennikov, S.V.; Vlassov, V.V.; Zenkova, M.A. Prophylactic Dendritic Cell-Based Vaccines Efficiently Inhibit Metastases in Murine Metastatic Melanoma. *PLoS ONE* **2015**, *10*, e0136911. [CrossRef]
39. Lorenzi, S.; Mattei, F.; Sistigu, A.; Bracci, L.; Spadaro, F.; Sanchez, M.; Spada, M.; Belardelli, F.; Gabriele, L.; Schiavoni, G. Type I IFNs Control Antigen Retention and Survival of CD8α^+ Dendritic Cells after Uptake of Tumor Apoptotic Cells Leading to Cross-Priming. *J. Immunol.* **2011**, *186*, 5142–5150. [CrossRef]
40. Zhou, H.; Forveille, S.; Sauvat, A.; Yamazaki, T.; Senovilla, L.; Ma, Y.; Liu, P.; Yang, H.; Bezu, L.; Müller, K.; et al. The Oncolytic Peptide LTX-315 Triggers Immunogenic Cell Death. *Cell Death Dis.* **2016**, *7*, e2134. [CrossRef]

41. Huang, B.; Sikorski, R.; Kirn, D.H.; Thorne, S.H. Synergistic Anti-Tumor Effects between Oncolytic Vaccinia Virus and Paclitaxel Are Mediated by the IFN Response and $HMGB_1$. *Gene Ther.* **2011**, *18*, 164–172. [CrossRef]
42. Schiavoni, G.; Mattei, F.; Gabriele, L. Type I Interferons as Stimulators of DC-Mediated Cross-Priming: Impact on Anti-Tumor Response. *Front. Immunol.* **2013**, *4*, 483. [CrossRef]
43. Lebon, A.; Tough, D. Type I Interferon as a Stimulus for Cross-Priming. *Cytokine Growth Factor Rev.* **2008**, *19*, 33–40. [CrossRef]
44. Wieczorek, M.; Abualrous, E.T.; Sticht, J.; Álvaro-Benito, M.; Stolzenberg, S.; Noé, F.; Freund, C. Major Histocompatibility Complex (MHC) Class I and MHC Class II Proteins: Conformational Plasticity in Antigen Presentation. *Front. Immunol.* **2017**, *8*, 292. [CrossRef] [PubMed]
45. Chow, A.; Toomre, D.; Garrett, W.; Mellman, I. Dendritic Cell Maturation Triggers Retrograde MHC Class II Transport from Lysosomes to the Plasma Membrane. *Nature* **2002**, *418*, 988–994. [CrossRef] [PubMed]
46. Veyer, D.L.; Carrara, G.; Maluquer de Motes, C.; Smith, G.L. Vaccinia Virus Evasion of Regulated Cell Death. *Immunol. Lett.* **2017**, *186*, 68–80. [CrossRef] [PubMed]
47. Kleinpeter, P.; Remy-Ziller, C.; Winter, E.; Gantzer, M.; Nourtier, V.; Kempf, J.; Hortelano, J.; Schmitt, D.; Schultz, H.; Geist, M.; et al. By Binding CD80 and CD86, the Vaccinia Virus M2 Protein Blocks Their Interactions with Both CD28 and CTLA4 and Potentiates CD80 Binding to PD-L1. *J. Virol.* **2019**, *93*, e00207-19. [CrossRef]
48. Engelmayer, J.; Larsson, M.; Subklewe, M.; Chahroudi, A.; Cox, W.I.; Steinman, R.M.; Bhardwaj, N. Vaccinia Virus Inhibits the Maturation of Human Dendritic Cells: A Novel Mechanism of Immune Evasion. *J. Immunol.* **1999**, *163*, 6762–6768.